HUNGARIAN AGRICULTURAL ENGINEERING
N° 39/2021 54-64
Published online: http://hae-journals.org/
HU ISSN 0864-7410 (Print) / HU ISSN 2415-9751(Online)
DOI: 10.17676/HAE.2021.39.54
Received: 03.05.2021 - Accepted: 26.05.2021

PERIODICAL
OF THE COMITTEE OF AGRICULTURAL AND BIOSYSTEM ENGINEERING OF THE HUNGARIAN ACADEMY OF SCIENCES
and
HUNGARIAN UNIVERSITY OF AGRICULTURE AND LIFE SCIENCES INSTITUTE OF TECHNOLOGY

HUNGARIAN UNIVERSITY OF AGRICULTURE AND LIFE SCIENCES
Institute of Technology

STEPPER MOTOR CONTROL SYSTEM FOR XY MODULE FOR IC PRODUCTION

Author(s):
E. Shibalkina[1,2], I. Szabó[1]

Affiliation:
[1] Institute of Technology, Hungarian University of Agriculture and Life Science (MATE), 2100 Gödöllő, Páter Károly u. 1., Hungary
[2] Doctoral School of Mechanical Engineering, Institute of Technology, Hungarian University of Agriculture and Life Science (MATE), 2100 Gödöllő, Páter Károly u. 1., Hungary

Email address:
e.shibalkina12@gmail.com; Szabo.Istvan.prof@uni-mate.hu

Abstract: The presented in the paper control system of the stepper motor of the two-coordinate printing module is developed on the basis of modern elements and allows you to control the stepper motor, providing the required shaft rotation speed and adjusting the number of rotation steps. This system realizes the processing of a moving object in several coordinates simultaneously without kinematic elements that convert rotary motion into linear, which makes it possible to speed up the time and accuracy of the processing tool. A forked optical sensor is used as workpiece position sensors. UART and USB bus are used for communication with the computer.

Keywords: stepper motor, simulation model, two-axis module.

1. Introduction

Stepper motors have taken a wide niche in industry and process control. Due to the simple principle of operation, which provides the necessary controllability without additional equipment. Stepper motors provide precise control of motor speed, angular position and direction of rotation of the motor. The stepper motor is best suited for the automation of individual units, modules and systems where high reliability and accuracy are required. Although stepper motors have been used for quite a long time, the popularity gained over the past several decades is due to the development of electronics. That in turn allows the creation of cheap and reliable control circuits meeting the complex requirements of motor speed, torque and angular displacement. In cases requiring positioning and precise speed control, as well as adjustable torque, a stepper motor is the most economical solution [1]

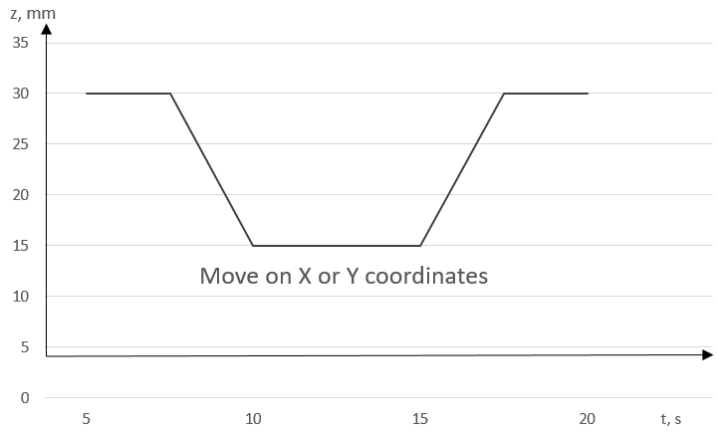

Figure 1. Diagram of the device operation.

The essence of the stepper motor is that the sequential activation of the motor windings generates discrete angular displacements (steps) of the rotor, and the angle of rotation of the rotor is determined by the number of pulses that are fed to the motor, which ensures the performance of the specified actions and their repeatability. Low rotational speeds for a load connected directly to the motor shaft can be obtained without an intermediate gear. Since the speed is proportional to the frequency of the input pulses, a fairly large speed range can be covered.

This paper presents a modular control system of stepper motor based microcontroller series ATMega 48 for a two-axis module for the production of integrated circuits.

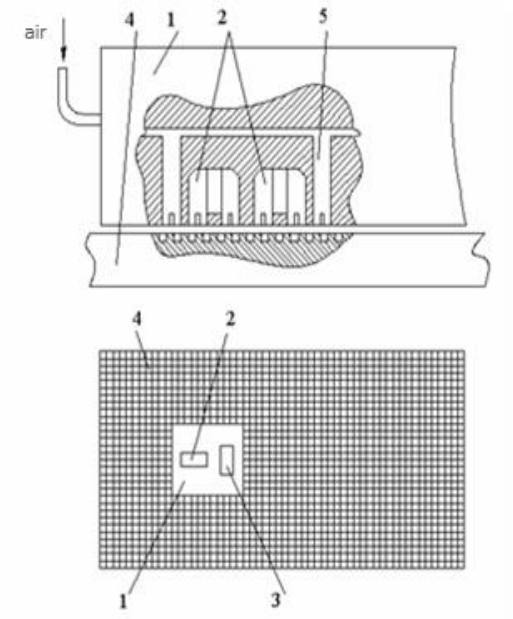

Figure 2. Coordinate table with a linear stepper motor: a) structural diagram; b) coordinate table with combined stator cutting: 1 - movable carriage, 2 - linear stepper motor of the X axis, 3 - linear stepper motor of the Y axis, 4 - stator, 5 – nozzles

2. Control Object and principle of operation

The control object (CO) is a two-coordinate transport module based on linear stepper motors (LSM), which is the main part of the probe installation used to manufacture microcircuits of a high integration degree.
The probe unit serves for marking the contact zones of the plate used for the manufacture of the microcircuit. The plate is divided into contact zones (80x80 microns), which are marked with a special paint in order to distinguish the defective contact zone from the working one.

The operating cycle of the installation is as follows. The coordinate table with the plate is raised until the position sensor (movement along the Z coordinate) is triggered, located 300 μm below the surface of the probes. After this sensor is triggered, the coordinate table moves along the Z coordinate at a lower speed to ensure smooth contact of the surface of the contact zone with the probes. The number of probes can be different: from 8 to 16. After marking the corresponding contact area, the XY table is lowered down to a height of 15 mm. After that, the coordinate table moves along the X or Y coordinate to move the next contact zone to the position directly below the probes. Then the XY table rises again and the next contact area is marked.

Coordinate systems that implement the movement of the processing object along several coordinates simultaneously without kinematic elements for converting rotary motion into translational motion are built on the basis of linear stepper motors.

Estimated system requirements

- simultaneous control of two stepper motors with a maximum phase current of up to 5.5 A;
- crushing 6400 microsteps per revolution;
- range of movement ±2147483648 discrete (step division);
- the maximum movement is up to ±8388608 discrete (step division).

The stepper motor control system is designed to generate signals on the stepper motor windings and control the rotation speed of its shaft and control the number of turning steps.

3. Control System and SIMULINK Model of the probe installation.

The stepper motor control system is designed to generate signals on the stepper motor windings and control the rotation speed of its shaft and control the number of turning steps.

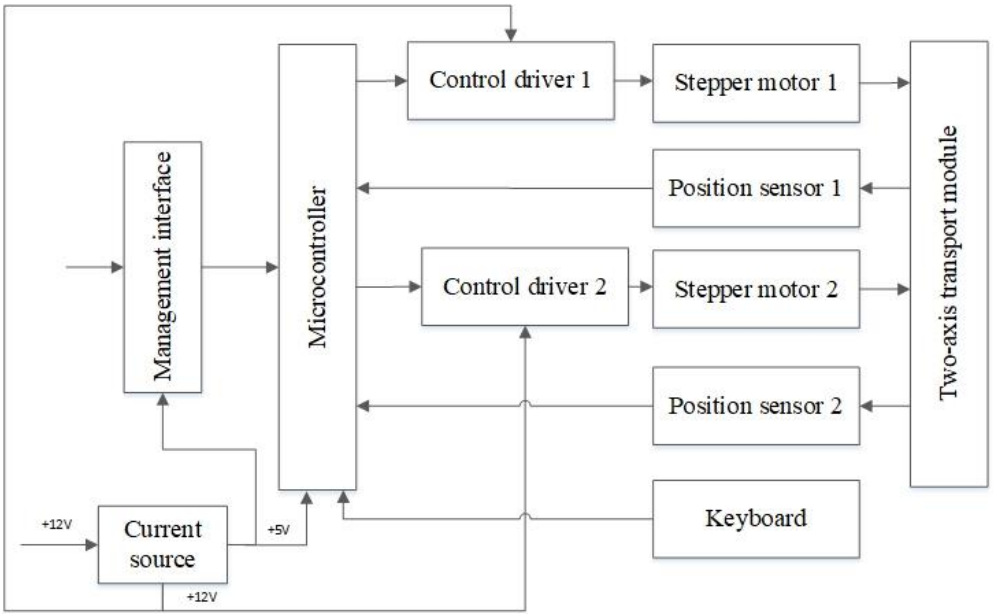

Figure 3. Block diagram of a stepper motor control system

Presented stepper control system (Figure3) has a separate controller and driver. This is due to the fact that a properly designed driver has a rather complex step crushing algorithm, which makes it possible to reduce the value of the minimum movement and avoid resonance phenomena. This separation makes it easy to use both specialized controllers made for a narrow range of tasks and the LPT port of a personal computer to control a stepper electric drive. The stepper motor driver for the user is a universal device, to the input of which only the power supply for the motor and the standard "direction" and "step" signals are supplied. On the driver, only the current value in the motor phases and the step division factor are set.

Motor control commands can be received via one of two communication interfaces either via USB or via UART, while the choice between one of these interfaces is carried out by switching the corresponding four microswitches, also installed on the board.

The control module is implemented on the AVR ATMega48 microcontroller, combined with the L6205 driver, which allows to control the drive based on both a stepper motor and a DC motor. The controller operates with a clock frequency of 10 MHz, with a supply voltage of + 5V. The USB interface is implemented on the basis of the FTDI FT232R converter, which allows quick pairing of standard UART and USB interfaces. To track the initial (zero) position of the motor shaft, an optical slot zero-mark sensor manufactured by Honeywell HOA08 is installed on the board. This sensor allows to unambiguously determine the initial position of the motor shaft when the supply voltage is reapplied or the microcontroller program is reset. The microcontroller's stable supply voltage is supported by the LM2594M pulsed buck DC-DC converter.

The module is connected to a standard USB port of a personal computer, via a cable with a mating miniUSB connector, or via a UART serial interface to another microprocessor system, while the signal level is + 5V. For programming the microcontroller, an ISP interface is provided, with contact pads for connecting a standard AVR programmer. It should also be noted that an LED connected directly to the controller is installed on the module to display the current operating mode or indicate an error. The typical supply voltage of the control system is + 12V, while its minimum level is slightly more than 8V and is limited to 20V.

3.1 Algorithm of the stepper motor control system

The algorithm of the main program (Figure 4) controls the speed of rotation of the stepper motor shaft and controls the number of steps of rotation. This algorithm is identical for engine 1 and engine 2.

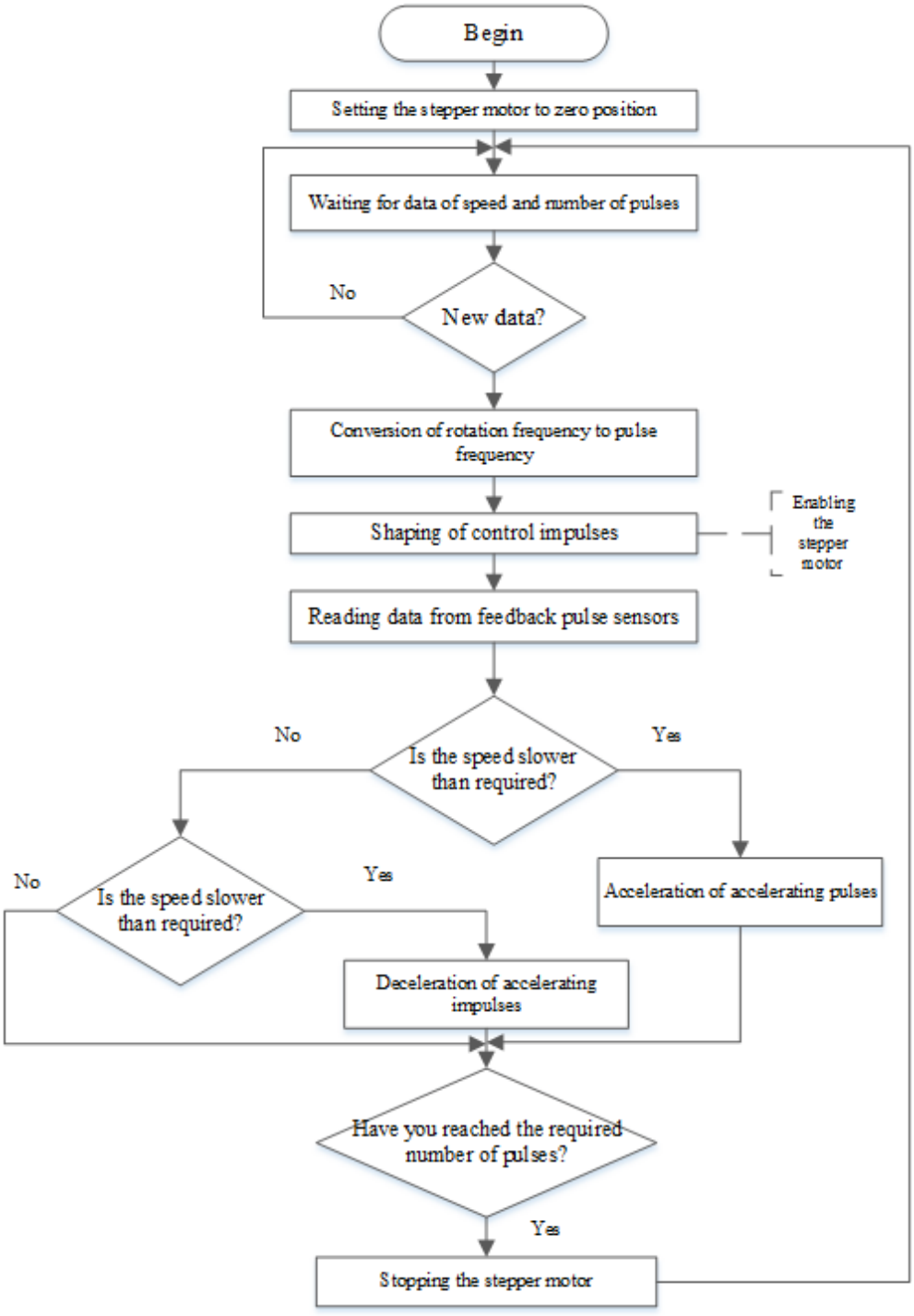

Figure 3. Algorithm of the stepper motor control system

3.2 The mathematical model of a stepper motor

The automated electric drive of the designed installation includes two two-phase linear stepper motors. Each phase is controlled by a control device that includes a current regulator and an inverter. The mathematical model of a stepper motor is described by the following equations:

$$u_A = R \times i_A + L \times \frac{di_A}{dt} + \Psi_m \times \frac{d\theta}{dt} \times \sin\theta$$
$$u_B = R \times i_A + L \times \frac{di_B}{dt} + \Psi_m \times \frac{d\theta}{dt} \times \cos\theta \quad (1)$$
$$\frac{d^2\theta}{dt^2} - k \times i_A \times \sin\theta - k \times i_B \times \cos\theta = f_l$$

Where A and B are the phases of the linear stepper motor; u_A and u_B - instantaneous values of voltages applied to phases; B - active resistance of the phase winding, Ω; A - phase winding inductance, H; i_A and i_B - instantaneous values of phase currents; Ψm - maximum flux linkage, Wb; θ - moving; m - moment constant, N / m; l - load force, N.

When simulating a stepper motor, it is necessary to take into account the holding torque (force) of the motor and the effect of the viscosity overcome by the rotor. In an inductor stepper motor with permanent magnets, the influence of the fourth harmonic of the torque (force), which is called the holding torque (force), is significant. This harmonic component should be taken into account by introducing an additional component at the load moment. The viscosity is also taken into account by the introduction of an additional component at the loading moment.

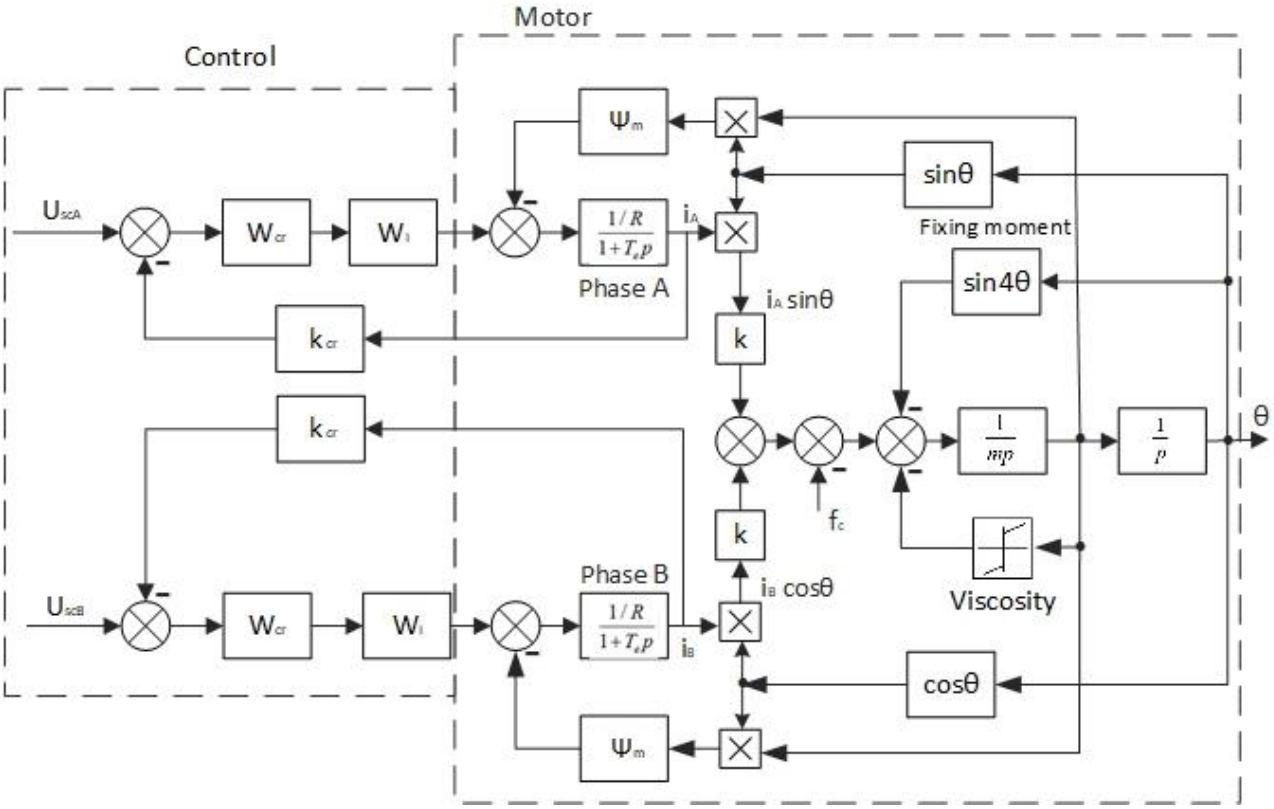

Figure 6. Diagram of an automated electric drive with a linear stepper motor

W_{cr} - is the transfer function of the current regulator;
W_i - transfer function of the inverter;
e - is the time constant of the winding of the motor phase;
U_{scA}, U_{scB} - signals for setting the currents of phases A and B, respectively.
The control object is a two-phase linear stepper motor.

3.3 Calculation of the parameters of the control object.

Motor phase winding time constant:

$$T_e = \frac{L}{R} = \frac{0.3\times10^{-3}}{5} = 0.06\text{ms} \quad (2)$$

Since the engine is running without load, the load force is l = 0.
Maximum flux linkage:

$$\Psi_m = L \times I_m \quad (3)$$

Where I_m is the maximum current in the motor phase.
Then, the maximum flux linkage:

$$\Psi_m = 0.3\times10^{-3}\times5.5 = 1.65\mu Wb \quad (4)$$

Technical characteristics of the Controlled Object:

Parameters	Values
Phase winding resistance, Ohm	5
Phase winding inductance, mH	0,3
Rotor weight, kg	3
Maximum flux linkage, Wb	0,00165
Fixing torque component, N / A	0,01
Viscous friction coefficient, Nm*s	10-4
Dry friction coefficient	10-8
Time constant of the winding of the motor phase, ms	0,06

The designed system requires a control system with a structure that has low sensitivity to parametric disturbances. To design such a structure, it is necessary to use the stability property with infinite gain in the loop.

To determine the stability conditions for a closed-loop system with an infinite gain β, we represent its characteristic polynomial in the form:

$$N(p) = a_n p^n + a_{n-1}p^{n-1} + ... + a_1 p + a_0 + \beta(b_m p^m + b_{m-1}p^{m-1} + ... + b_0) \quad (5)$$

In formula (5), the following designations are adopted: b_i are the coefficients expressed in terms of the parameters of the system.

In accordance with the conditions of M. V. Meerov [2] for

n - m = 1 the system remains stable at $\beta \to \infty$ always, at

n - m = 2 subject to inequality $a_{n-1}/a_n > b_{m-1}/b_m$ and in case n - m $\geq$ 3 at $\beta \to \infty$ the system does not remain stable.

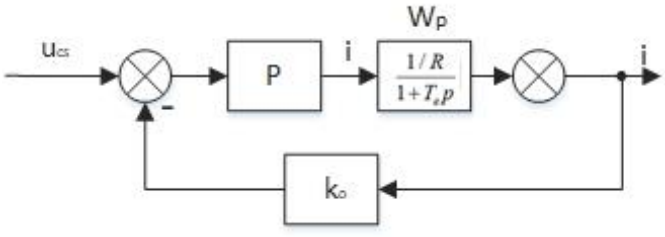

Figure 7. Current regulation loop

Figure 7 shows a current control loop, in the forward channel of which there is a link P. Its input-output characteristic has a vertical section equivalent to infinite gain, and the output signal u is limited in magnitude by the value um. If we denote by β the gain of the link P, then the transfer function of the circuit can be represented as:

$$\Phi = x(p)/u(p) = \beta W/(1+k_0\beta W) \tag{6}$$

Obviously

$$\lim_{\beta\to\infty}\Phi = 1/k_0 \tag{7}$$

and the contour properties do not depend on the link parameters W(p). So, for

$$W(p) = \frac{k}{T_e p+1} \tag{8}$$

we get:

$$\Phi = \beta k(1+T_e p+k_0 k\beta) \tag{9}$$

n = 1, m = 0, n - m = 1, and the system is stable at $\beta \to \infty$.

Since all the conditions for using the relay regulator are met, we implement the current regulator with a relay element with the maximum permissible deviation of the actual phase current from the reference current equal to 0,05A (1% from rated current 5,5 A).

3.4 Simulation model

Computer modelling of the projected installation performed in the MATLAB 6.0 mathematical modelling environment using the Simulink library. The model is based on Equations 1.

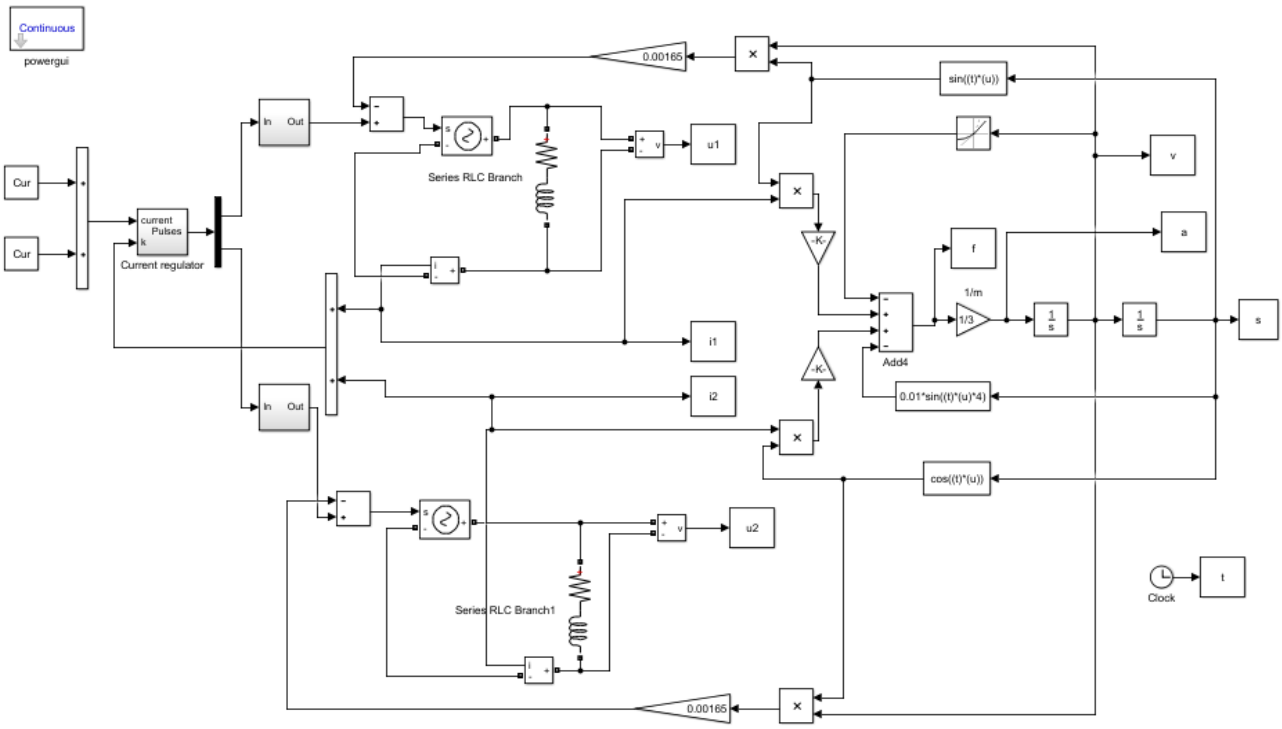

Figure 8. Simulation model of the electric drive of the designed installation.

Where

a and La - resistance and inductance of the winding of phase A;

в and Lв - resistance and inductance of the winding of phase B;

Blocks "u1" and "u2" return the time dependences of voltages applied to phases A and B; blocks "i1" and "i2" return the currents of phases A and B as a function of time; block "f" returns the linear stepper motor traction as a function of time; block "a" returns the acceleration as a function of time; block "v" - returns the speed as a function of time; the "s" block returns the movement as a function of time. The block "1 / m" takes into account the mass of the moving part, equal to 3 kg.

4. Simulation Results

The graphs obtained as a result of modeling in the MATLAB environment are presented in Figures 9-17.

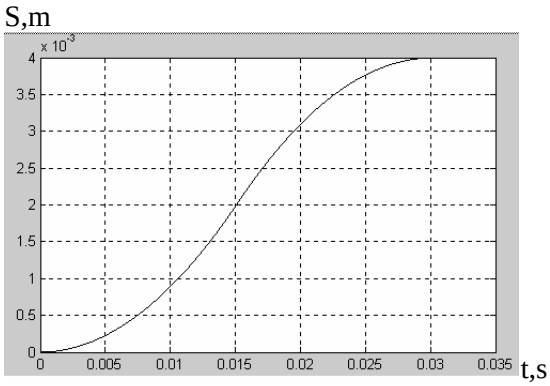

Figure 9. Displacement as a function of time

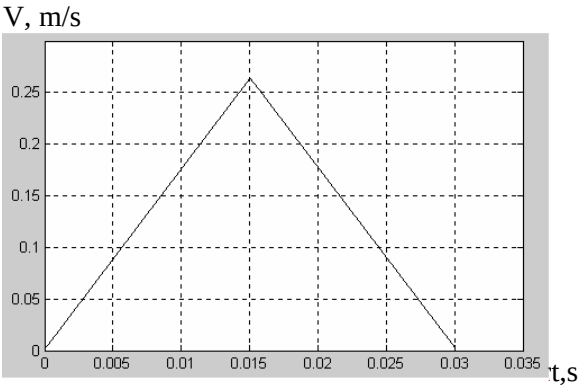

Figure 10. Speed as a function of time

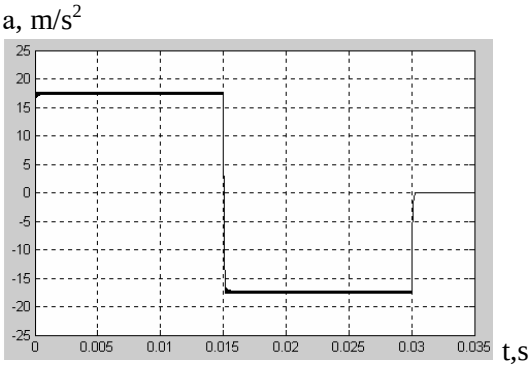

Figure 11. Acceleration as a function of time

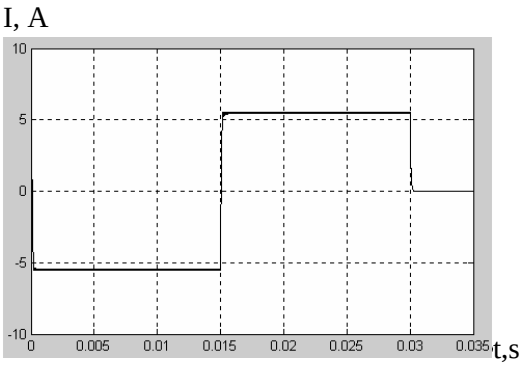

Figure 12. Phase A current as a function of time

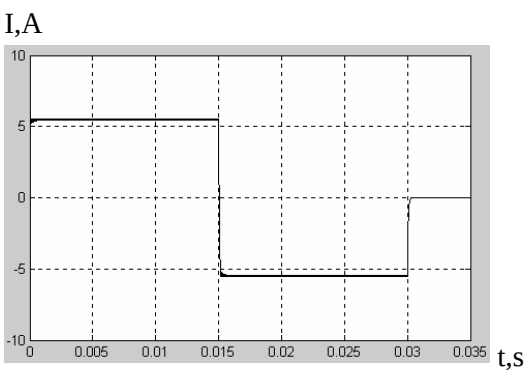

Figure 13. Phase B current as a function of time

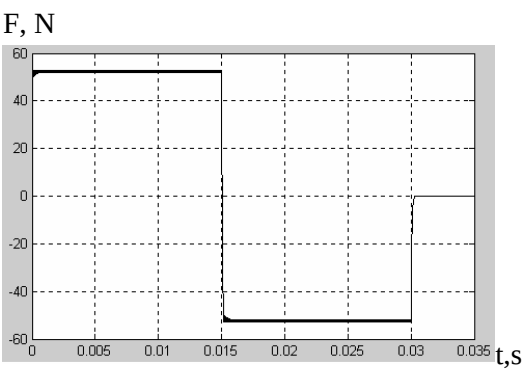

Figure 14. Tractive effort as a function of time

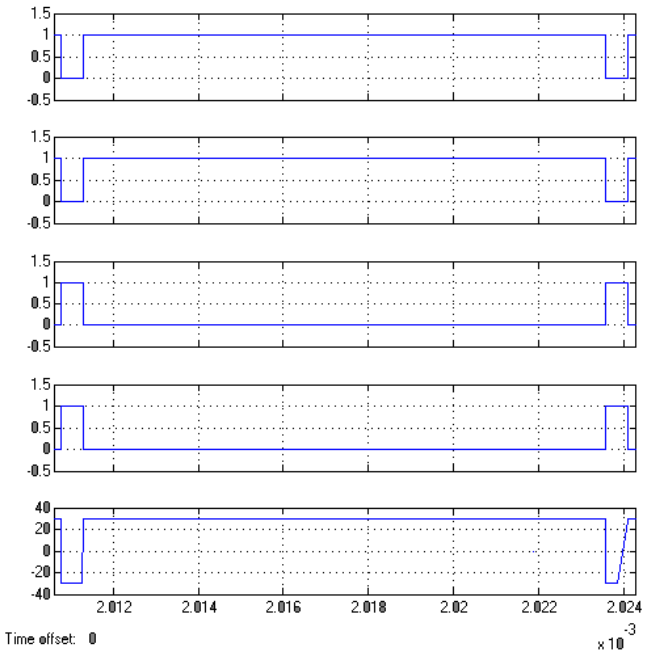

Figure 15. Algorithm of operation of the switches of the phase A inverter

Figure 15 shows the algorithm of operation of the switches of the phase A inverter for a time from 2.01*10-3 s to 2.025*10-3 s. This is the time period in the acceleration section of the electric motor. Since the frequency of the pulse-width modulation of the voltage is very high, due to the fact that the permissible deviation of the phase current from the given one is 1%, it is impossible to reliably reflect the change in voltage on the phase of the electric motor throughout the entire time of a typical movement. The algorithm of operation of the switches of the phase B inverter is shown in Figure 16.

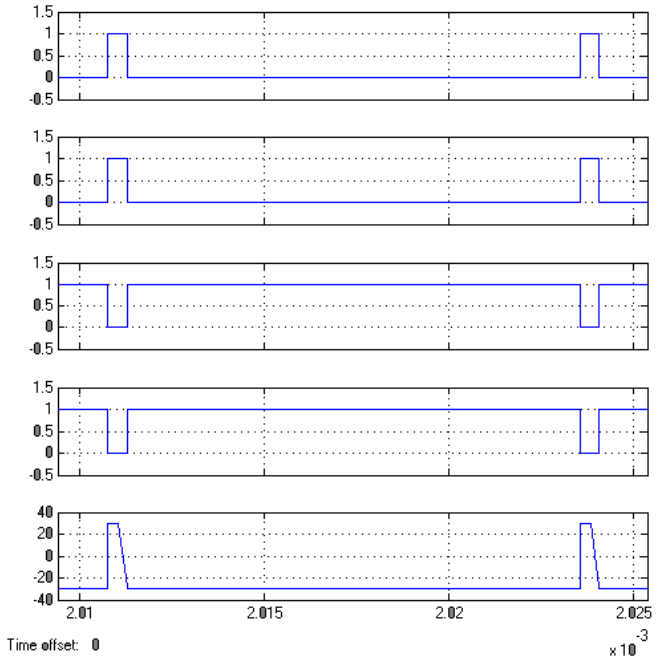

Figure 16. Algorithm of operation of the switches of the phase B inverter

The phase B current command signal is out of phase with respect to the phase A current command signal by 90 electrical degrees.

4.1. Calculation overshoot

The quality of regulation is usually assessed by the following main indicators [8]:
- the amount of overshoot;
- speed or time of regulation;
- the number of fluctuations of the controlled value during the transient process.

The overshoot is calculated by the formula:

$$\Delta\% = \frac{h_{\max} - h_{set}}{h_{set}} \times 100\% \tag{10}$$

Positional overshoot is especially important for the plant being designed.

Diagram on Figure 17 shows that $h_{max} = h_{set} = 4$ mm, therefore, overshoot Δ % = 0%. When working out a single step $h_{max} = h_{set} = 10$ μm .The response speed, or regulation time, is the time during which the deviation of the controlled value from the steady-state value exceeds a certain permissible value. In most cases, this value is assumed to be 5%. From Figures 9 and 17 it is obvious that the controlled variable (displacement) after reaching the steady-state value no longer deviates from it, and, therefore, the regulation time is zero.

The number of fluctuations of the controlled value during the transient process does not exceed the permissible value, since there are no fluctuations.

Figure 17 shows that the unit step size is 10 μm, therefore, the system meets the requirements for positioning accuracy. Figure 10 shows that the maximum speed in the designed installation is 0.27 m /s, which doesn't exceed the required maximum speed of 0.28 m /s and is equal to the value of the calculated maximum speed.

Figure 11 shows that the maximum acceleration is 17.7 m /s^2, which does not exceed the required value of 18 m /s^2.

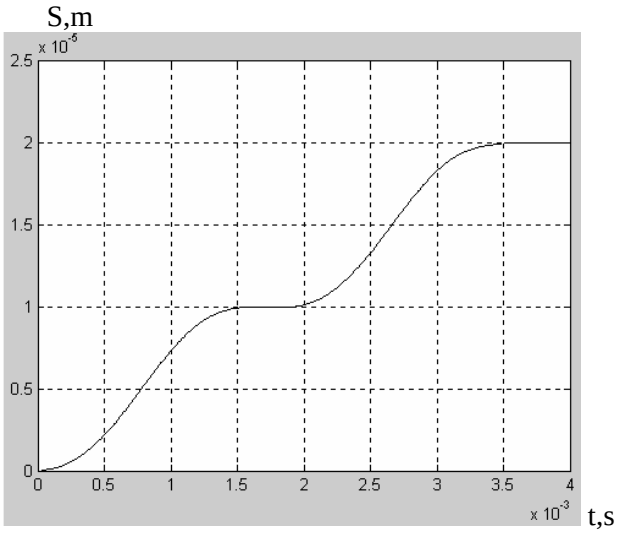

Figure 17. Diagram of the stepper motor working out two steps forward.

4. Conclusion

Currently, a good alternative to micro-drives, consisting of a high-speed feedback motor and a manual transmission, is the stepper drive, which has already become a traditional actuator for many electronic devices and systems.

In particular, the system is attractive in that it is small in size, provides engine protection when operating in critical modes, and is easy to configure.

Acknowledgement

Special thanks to the Stipendium Hungaricum Scholarship Programme, Institute of Technology and the Mechanical Engineering Doctoral School, Hungarian University of Agriculture and Life Sciences, Gödöllő, Hungary.

References

[1] B.S. Somesh, A. Mukherjee, S. Sen, P. Karmakar: (2014) Constant Current Control of Stepper Motor in Microstepping Mode using PIC16F877A, Devices, Circuits and Systems (ICDCS), 2014, 2nd International Conference, pp.1-4.

[2] D.P. Atherton, G.W. Irwin (2007) "Stepping Motors a guide to theory and practice", 4th Edition, The institute of Enginering and Technology,.

[3] Gorunov N. N (2007) Handbook of semiconductor devices and integrated circuits. 4th Edition, rev. and add. M.: "Energy".

[4] Hoang Le-Huy, Brunelle P., Sybille G. (2008) Design and Implementation of a Versatile Stepper Motor Model for Simulink's SimPowerSystems, IEEE International Symposium on Industrial Electronics, 2008, ISIE 2008, pp- 437-442.

[5] M. Bendjedia, Y. Ait-Amirat, B. Walther, A. Berthon (2012) Position Control of a Sensorless Stepper Motor, IEEE Trans. Power Electronics, vol. 27, no. 2, pp. 578-587.

[6] M. Bendjedia, Y. Ait-Amirat, B. Walther, A. Berthon: (2012) Position Control of a Sensorless Stepper Motor, IEEE Trans. Power Electronics, vol. 27, no. 2, pp. 578-587.

[7] T. Kenjo: (1983) Stepping Motors and Microprocessor Control, London: Oxford Clarendon Press.

[8] W. Kim, D. Shin, C.C. Chung (2013) Microstepping With Nonlinear Torque Modulation for Permanent Magnet Stepper Motors, IEEE Trans. Control Systems Technology, vol. 21, no. 5, pp. 1971-1979.